Molecular Therapy
Nucleic Acids
Original Article

Circulating extracellular vesicles promote recovery in a preclinical model of intracerebral hemorrhage

Fernando Laso-García,[1,2,7] Laura Casado-Fernández,[1,7] Dolores Piniella,[1,3,7] Mari Carmen Gómez-de Frutos,[1] Jone Karmele Arizaga-Echebarria,[1] María Pérez-Mato,[1] Elisa Alonso-López,[1] Laura Otero-Ortega,[1] Susana Belén Bravo,[4] María del Pilar Chantada-Vázquez,[4] José Avendaño-Ortiz,[5] Eduardo López-Collazo,[5] María Isabel Lumbreras-Herrera,[6] Angelo Gámez-Pozo,[6] Blanca Fuentes,[1] Exuperio Díez-Tejedor,[1] María Gutiérrez-Fernández,[1,8] and María Alonso de Leciñana[1,8]

[1]Neurological Sciences and Cerebrovascular Research Laboratory, Department of Neurology and Stroke Centre, Neurology and Cerebrovascular Disease Group, Neuroscience Area Hospital La Paz Institute for Health Research – IdiPAZ (La Paz University Hospital- Universidad Autónoma de Madrid), Madrid, Spain; [2]PhD Program in Neuroscience, Autónoma de Madrid University-Cajal Institute, Madrid 28029, Spain; [3]Universidad Autónoma de Madrid and IdiPAZ Health Research Institute, La Paz University Hospital, Madrid, Spain; [4]Proteomic Unit, Health Research Institute of Santiago de Compostela (IDIS), Santiago de Compostela, Spain; [5]TumorImmunology Laboratory and Innate Immune Response Group, IdiPAZ Health Research Institute, Madrid, Spain; [6]Molecular Oncology and Pathology Lab, Institute of Medical and Molecular Genetics-INGEMM, La Paz University Hospital-IdiPAZ, Madrid, Spain

Circulating extracellular vesicles (EVs) are proposed to participate in enhancing pathways of recovery after stroke through paracrine signaling. To verify this hypothesis in a proof-of-concept study, blood-derived allogenic EVs from rats and xenogenic EVs from humans who experienced spontaneous good recovery after an intracerebral hemorrhage (ICH) were administered intravenously to rats at 24 h after a subcortical ICH. At 28 days, both treatments improved the motor function assessment scales score, showed greater fiber preservation in the perilesional zone (diffusion tensor-fractional anisotropy MRI), increased immunofluorescence markers of myelin (MOG), and decreased astrocyte markers (GFAP) compared with controls. Comparison of the protein cargo of circulating EVs at 28 days from animals with good vs. poor recovery showed down-expression of immune system activation pathways (CO4, KLKB1, PROC, FA9, and C1QA) and of restorative processes such as axon guidance (RAC1), myelination (MBP), and synaptic vesicle trafficking (SYN1), which is in line with better tissue preservation. Up-expression of PCSK9 (neuron differentiation) in xenogenic EVs-treated animals suggests enhancement of repair pathways. In conclusion, the administration of blood-derived EVs improved recovery after ICH. These findings open a new and promising opportunity for further development of restorative therapies to improve the outcomes after an ICH.

INTRODUCTION

Intracerebral hemorrhage (ICH) is the most devastating form of stroke, with a mortality rate up to 40% and the highest loss of disability-adjusted life years among survivors.[1,2] Each year, approximately 5 million people worldwide experience an ICH, two-thirds of whom will survive with a disability. However, specific treatments with demonstrated efficacy in improving outcomes are lacking, despite increasing knowledge of the pathological mechanisms involved in brain damage after ICH. There is also evidence that, beyond the injury cascades, mechanisms of protection and repair are triggered after an ICH.[3,4] A deeper understanding of these mechanisms is a promising approach that may lead to the development of treatments aimed at improving neurological recovery by enhancing brain plasticity. In this regard, animal studies have demonstrated that stem cell-based therapies reduce brain injury and improve recovery after ICH.[5–7] Preclinical studies have also shown that cell therapy enhances brain plasticity through the release of soluble trophic factors and other molecules[8–10] and emerging data suggest that these paracrine effects of stem cell therapy could be exerted by the release of extracellular vesicles (EVs).[11] EVs are known to be secreted by most cell types and can be found in blood and other body fluids.[12,13] These EVs carry bioactive molecules (proteins, lipids, and various types of RNA)[14] that participate in intercellular signaling and can modulate physiological functions.[14,15] Studies have demonstrated

Received 10 December 2022; accepted 16 March 2023;
https://doi.org/10.1016/j.omtn.2023.03.006.

[7]These authors contributed equally

[8]These authors contributed equally

Correspondence: María Gutiérrez-Fernández, Neurological Sciences and Cerebrovascular Research Laboratory, Department of Neurology and Stroke Centre, Paseo de la Castellana, 261, 28046 Madrid, Spain.
E-mail: mgutierrezfernandez@salud.madrid.org
Correspondence: María Alonso de Leciñana, Neurological Sciences and Cerebrovascular Research Laboratory, Department of Neurology and Stroke Centre, Paseo de la Castellana, 261, 28046 Madrid, Spain.
E-mail: malecinanacases@salud.madrid.org

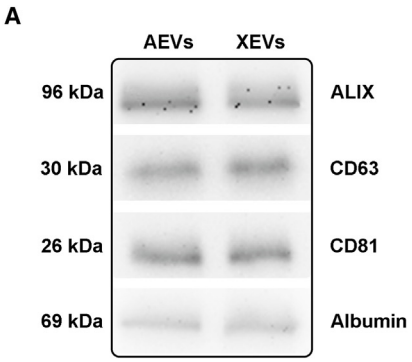

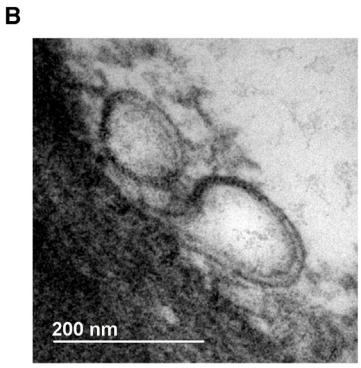

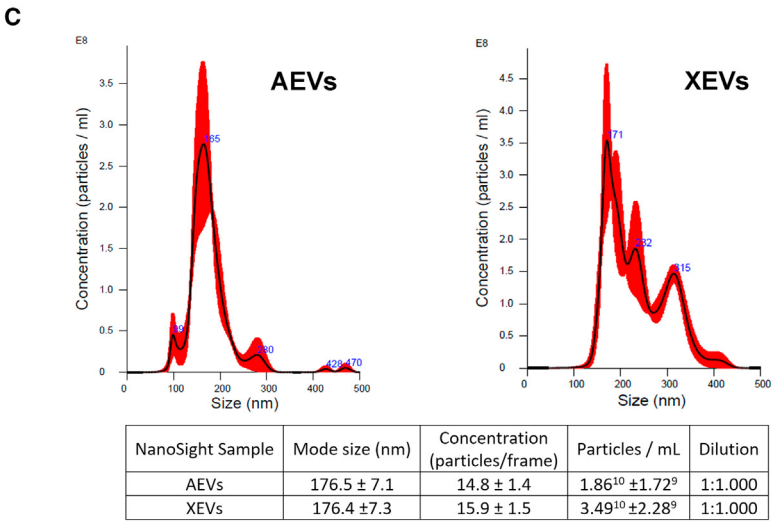

NanoSight Sample	Mode size (nm)	Concentration (particles/frame)	Particles / mL	Dilution
AEVs	176.5 ± 7.1	14.8 ± 1.4	1.86^{10} ±1.72^{9}	1:1.000
XEVs	176.4 ±7.3	15.9 ± 1.5	3.49^{10} ±2.28^{9}	1:1.000

Figure 1. Extracellular vesicles (EVs) characterization
(A) Presence of specific EVs markers (Alix, CD63, and CD81) and albumin as a purity control by western blot analysis after isolation. (B) Transmission electron microscopy (TEM) images showing the characteristic size and form of the EVs. (C) NTA showing the size and concentration of the EVs. AEVs, allogeneic extracellular vesicles; NTA, nanoparticle tracking analysis; XEVs, xenogenic extracellular vesicles.

that the intravenous administration of mesenchymal stem cell (MSC)-derived EVs promotes neurovascular plasticity and improves neurological recovery after ischemic and hemorrhagic stroke in rats.[16–22] EVs are therefore gaining interest as a potential approach to regenerative medicine for neurological diseases.

Our hypothesis is that endogenous mechanisms of protection and repair triggered after an ICH could be mediated by circulating EVs through their protein cargo. If so, the protein content of EVs from subjects showing a good recovery after an ICH might exert a beneficial effect if administered to animals subjected to an experimental ICH. Therefore, a proof-of-concept study is proposed in a rodent model of ICH in which the effect of intravenously administered blood-derived allogeneic or xenogenic EVs obtained from subjects (rats and humans, respectively) that had a spontaneous good recovery after an ICH, will be analyzed in terms of efficacy and safety comparing treated and non-treated animals. Moreover, by analyzing the protein content of circulating EVs from animals after treatment compared with controls, the study intends to delve into the signaling pathways potentially involved in the brain repair mechanisms after ICH. This is a novel approach that may help to advance the development of new treatments for cerebral hemorrhage.

RESULTS

Of the total 88 rats included in the study, nine died immediately after ICH induction (four in the control group, two in the allogeneic EV [AEV] group, and three in the xenogenic EV [XEV] group). One of the rats in the XEVs group died during treatment administration, and six were excluded because they showed no hemorrhage on the magnetic resonance imaging (MRI) (five in the control group and one in the AEVs group). The death rats and those excluded from the study were replaced by new subjects until the predefined number of rats per group with confirmed ICH by MRI at 48 h was reached.

EVs characterization

AEVs and XEVs showed typical protein markers by western blot (Figure 1A), morphology and size (<200 nm) by transmission electron microscopy (TEM) (Figure 1B) and nanoparticle tracing analysis (NTA) (Figure 1C).

Evolution of the rats in the control group

Outcomes of the rats in the control group are shown in Figure 2A and Table S1. Those rats with a spontaneous recovery, as defined in the materials and methods section, at 28 days (n = 7) were selected as donors of AEVs for treatment.

Efficacy of AEVs and XEVs administration

AEVs and XEVs treatment improves motor function after ICH

The motor recovery of the animals treated with AEVs and XEVs was significantly better than that of the control group, as shown in all tests used in the study (Figure 3A, Table S1).

AEVs and XEVs treatment was associated with white matter integrity in the MRI assessment

There were not significant differences in the volume of lesion in MRI at baseline nor at follow-up between the study groups (Figure 3B). The diffusion tensor imaging fractional anisotropy (DTI-FA) values were significantly higher in the treated animals

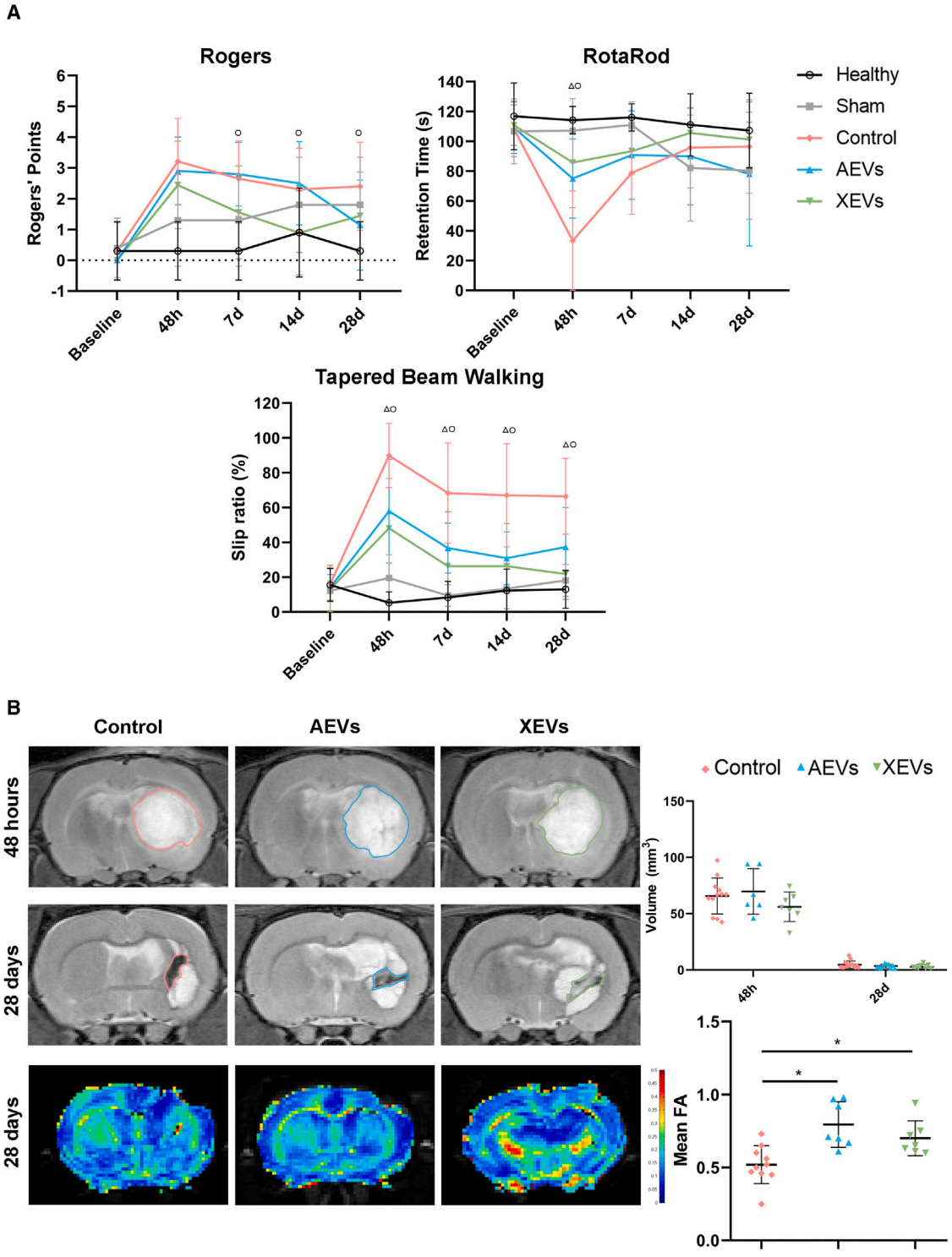

Figure 2. Functional evaluation and brain imaging

(A) Functional evaluation tests along the study time points. "Δ" indicates $p < 0.05$ in AEV-treated animals compared with the control group. "O" indicates $p < 0.05$ in the XEVs-treated animals compared with the control group. (B) T2-MRI images. Colored lines mark the total volume of lesion at 48 h and the residual lesion at 28 days surrounded by dilated cisterns as a result of tissue retraction. * indicates $p < 0.05$. Data are shown as mean ± SD. AEVs, allogeneic extracellular vesicles; FA, fractional anisotropy; ICH, intracerebral hemorrhage; XEVs, xenogenic extracellular vesicles.

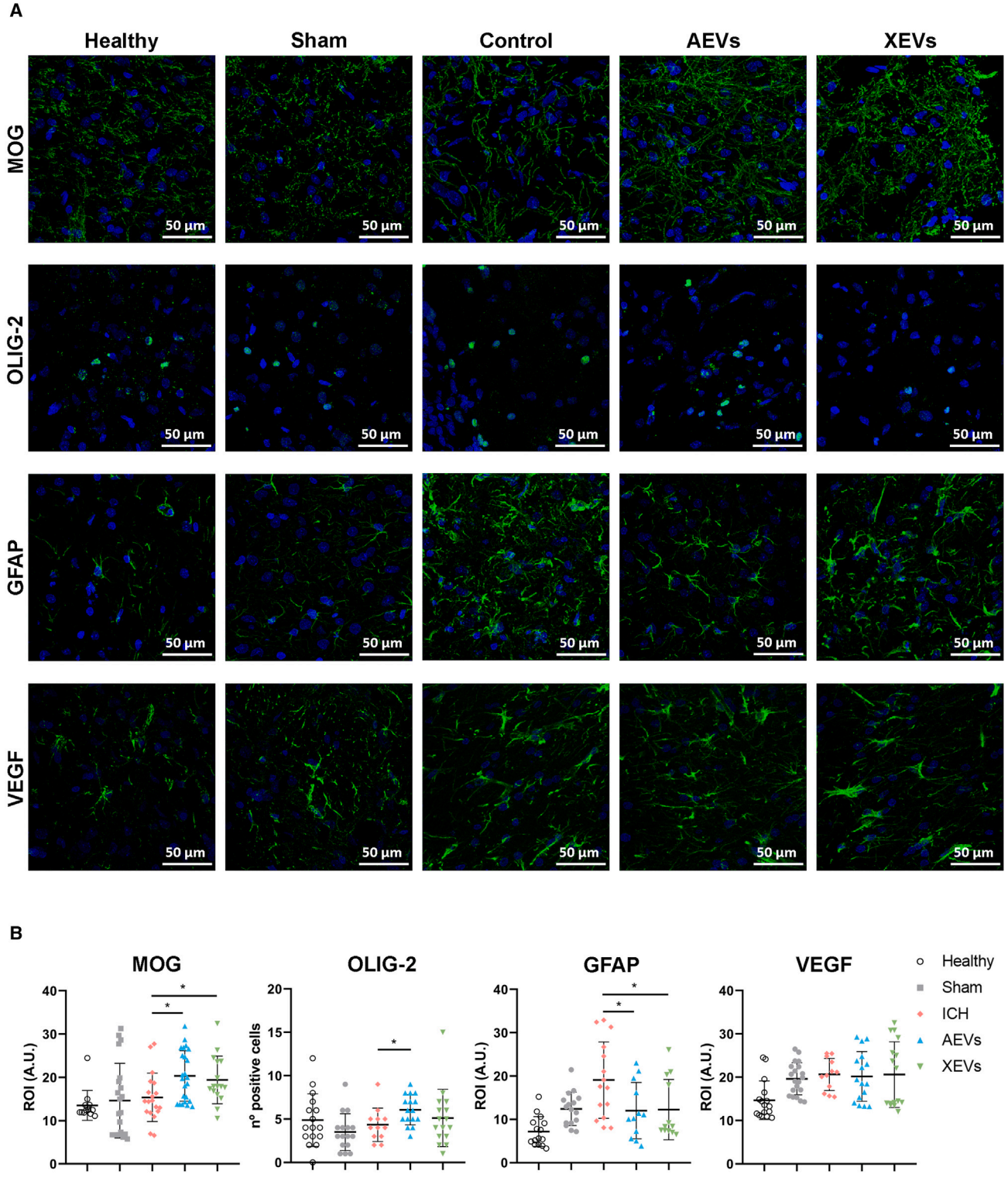

Figure 3. Signal detection of brain markers by immunofluorescence

(A) Myelin (MOG), oligodendrocytes (OLIG-2), astrocytes (GFAP), and vascular (VEGF) antibody expression. (B) Quantification of brain marker expression. * indicates $p < 0.05$. Data are shown as mean ± SD. AEVs, allogeneic extracellular vesicles; XEVs, xenogenic extracellular vesicles.

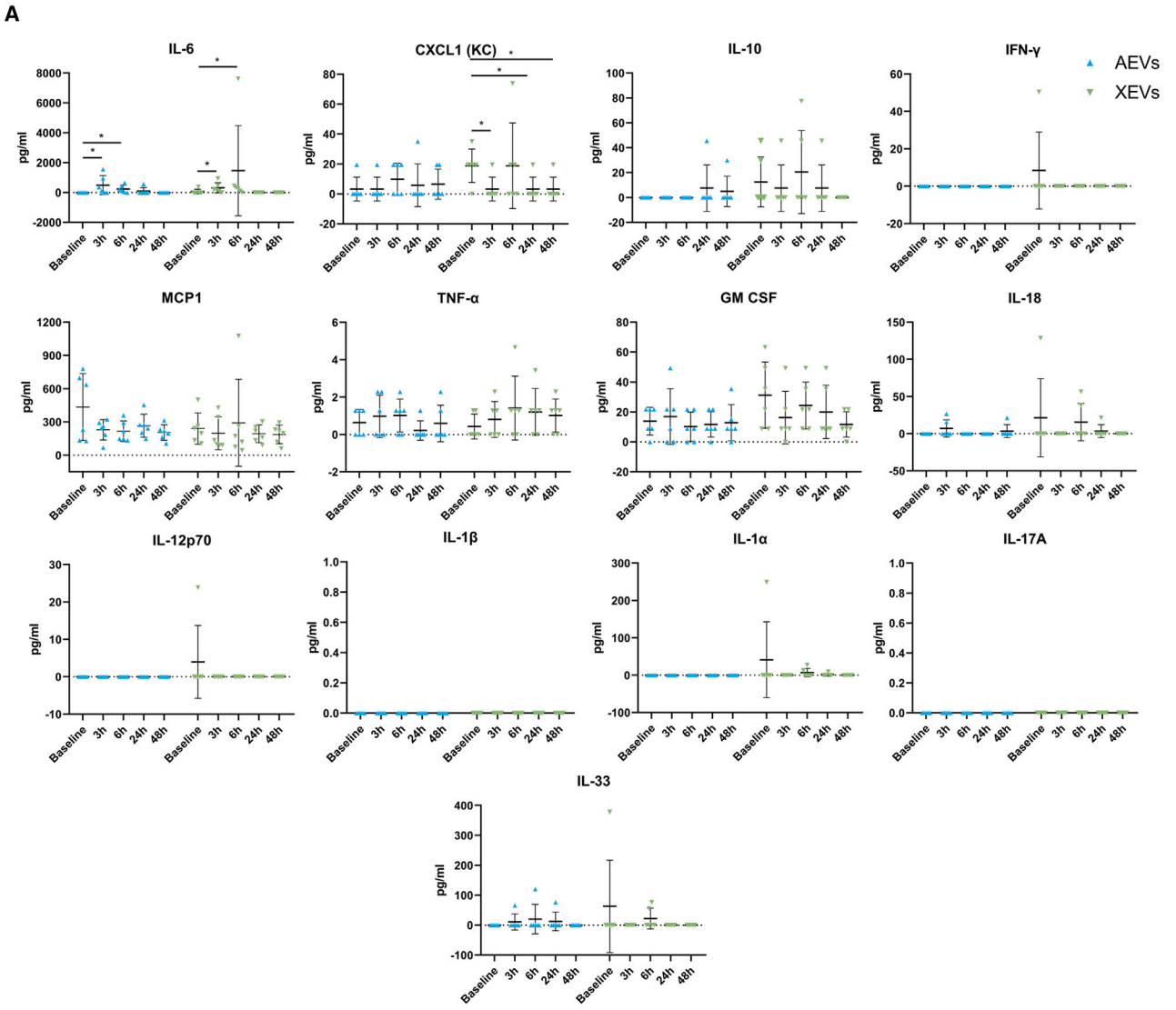

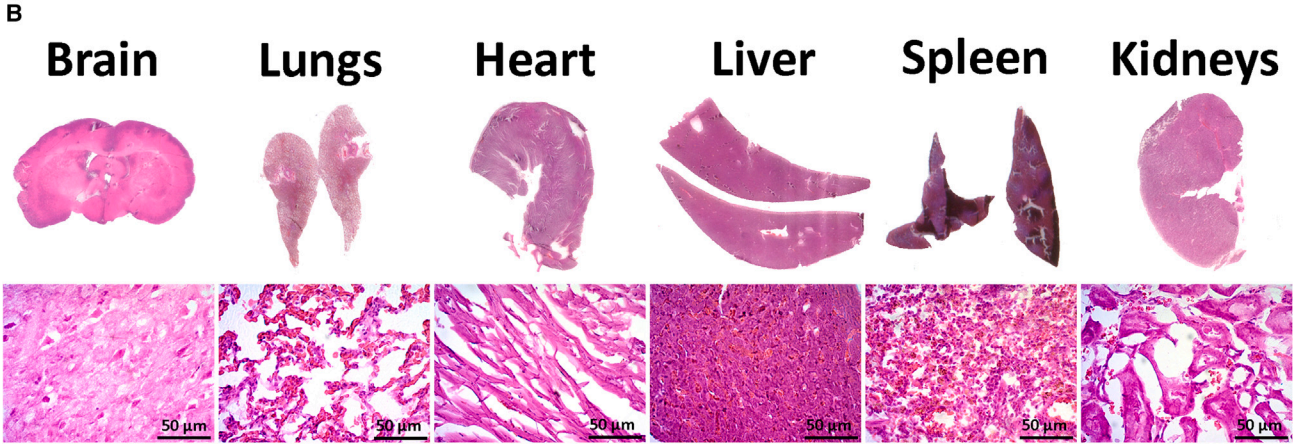

(legend on next page)

compared with the controls at 28 days, indicating greater white matter integrity after either AEVs or XEVs treatment (Figure 3B, Tables S2 and S3).

AEVs and XEVs improve histological markers of brain damage and repair

Figure 3 and Table S4 show the immunofluorescence analysis in the study groups. There was a significantly higher expression of myelin oligodendrocyte glycoprotein (MOG) in both treated groups compared with the control group. There was a significantly higher expression of oligodendrocyte transcription factor 2 (OLIG-2) antibody in the AEVs group than in the control group, but there were no significant differences between the XEVs and control groups. Glial fibrillary acid protein (GFAP) expression was significantly higher in the control group than in both treated groups. Vascular endothelial growth factor (VEGF) expression was uniform in all study groups, showing no statistically significant differences between groups.

Safety of administering AEVs and XEVs

Absence of immune system response or tumor formation

Thirteen cytokines and chemokines were analyzed in plasma from the rats treated with AEVs and XEVs (Figure 4A, Table S5). Only interleukin (IL)-6 showed a slight increase at 3 h and 6 h compared with baseline, returning to normal at later time points, whereas CXCL1 decreased at 3 h, 24 h, and 48 h compared with baseline in the XEVs-treated animals. There were no changes in the plasma levels of IL-10, interferon (IFN)-γ, MCP1, tumor necrosis factor (TNF)α, granulocyte-macrophage colony-stimulating factor (GM-CSF), IL-18, IL-12p70, IL-1β, IL-1α, IL-17A, or IL-33 after AEVs or XEVs administration.

The macroscopic and microscopic hematoxylin and eosin (H&E) examination of the organs revealed no signs of malignancy neoformations (Figure 4B).

Proteomics analysis of circulating EVs content in the treatment groups

The proteomic analysis of the circulating EVs obtained from blood samples at 28 days after the ICH in the study groups showed a total of 1,024 different proteins with a 1% error at the false discovery rate (FDR) threshold. The proteins found in each study comparison and the biological pathways, in which the differentially expressed proteins appear to be involved, are shown in Figure 5, Table S6. We focused on proteins and pathways potentially involved in mechanisms of damage and repair, such as immune response and inflammation, axon guidance, axonogenesis, synaptic vesicle trafficking, angiogenesis, neuron differentiation, and myelination. The main findings are summarized below.

Control animals with good vs. poor spontaneous recovery

Eight proteins showed significant differences according to the previous definition in the control animals with good spontaneous recovery compared with the control animals with poor spontaneous recovery (Figure 5A and Table S6). Of those proteins, two of them were up-expressed: leukemia inhibitory factor receptor (LIFR) and A1BG (platelet and neutrophil degranulation). Six proteins were down-expressed: FA9 and KLKB1 (coagulation factor and inflammatory response), RAC1 (axon guidance and angiogenesis), TRFE (cellular iron ion homeostasis), TTHY (thyroid hormone metabolic process and transport), and APOH (blood coagulation).

Treatment with AEVs vs. control groups

Six proteins showed significant differences as per the mentioned criteria between the AEVs and control groups (Figure 5B and Table S6). Three proteins were up-expressed: RL22 (RNA binding), and K2C5 and K2C73 (keratin cytoskeletal), and three proteins were down-expressed: CO4 (complement system), and IGG2C and IGHD (innate immune response).

Treatment with XEVs vs. control groups

Eighty-two proteins showed significant differences as per the mentioned criteria (Figure 5C and Table S6). The most significant proteins up-expressed in the XEVs group compared with the control group were C1S and CO4 (complement system); PROC, F13A, ZPI, THRB, HEP2, PROS, KNG1 and KNT2 (blood coagulation); CO9 (blood coagulation and complement system); IGHG1 (B cell receptor signaling pathway and complement system); C1QA (astrocyte activation and complement system); IGG2C (innate immune response); PLF4 (immune response); A1AT (inflammatory response); ALS (cell adhesion); KLKB1 (blood coagulation and inflammatory response); TRFE, SPA3N, HEMO, and CERU (cellular iron ion homeostasis); LIFR (leukemia inhibitory factor signaling pathway); HBA (erythrocyte development); TSP4 (negative regulation of angiogenesis); and PCSK9 (neuron differentiation). Meanwhile, MBP (myelination); SYN1 (synaptic vesicle trafficking); K2C73, K1C10 and K2C5 (keratin cytoskeletal); PLAK (cell adhesion); FIBA (blood coagulation); B2MG (innate immune response); and SYCP2 (cell division) were down-expressed.

Treatment with AEVs vs. treatment with XEVs

Seventy-five proteins showed significant differences between the two treated groups (Figure 5D and Table S6). The most significant proteins up-expressed in the AEVs group compared with the XEVs group were RL22 (T cell differentiation), K2C73 and K2C5 (keratin cytoskeletal), STX1A (synaptic vesicle trafficking), ZDH17 (axonogenesis), and AOFB (neurotransmitter metabolism). The most significant proteins found down-expressed were FA9 and FA10 (coagulation factor); CBPB2, PLMN, APOH, PROC, F13A, FA7, ZPI, KLKB1, HEP2,

Figure 4. Immune response evaluation

(A) Cytokine levels in rat plasma at baseline and at 3 h, 6 h, 24 h, and 48 h after treatment. (B) Macroscopic and microscopic examination of organs showed no signs of malignancy or neoformations. * indicates $p < 0.05$. Data are shown as mean ± SD. AEVs, allogeneic extracellular vesicles; XEVs, xenogenic extracellular vesicles.

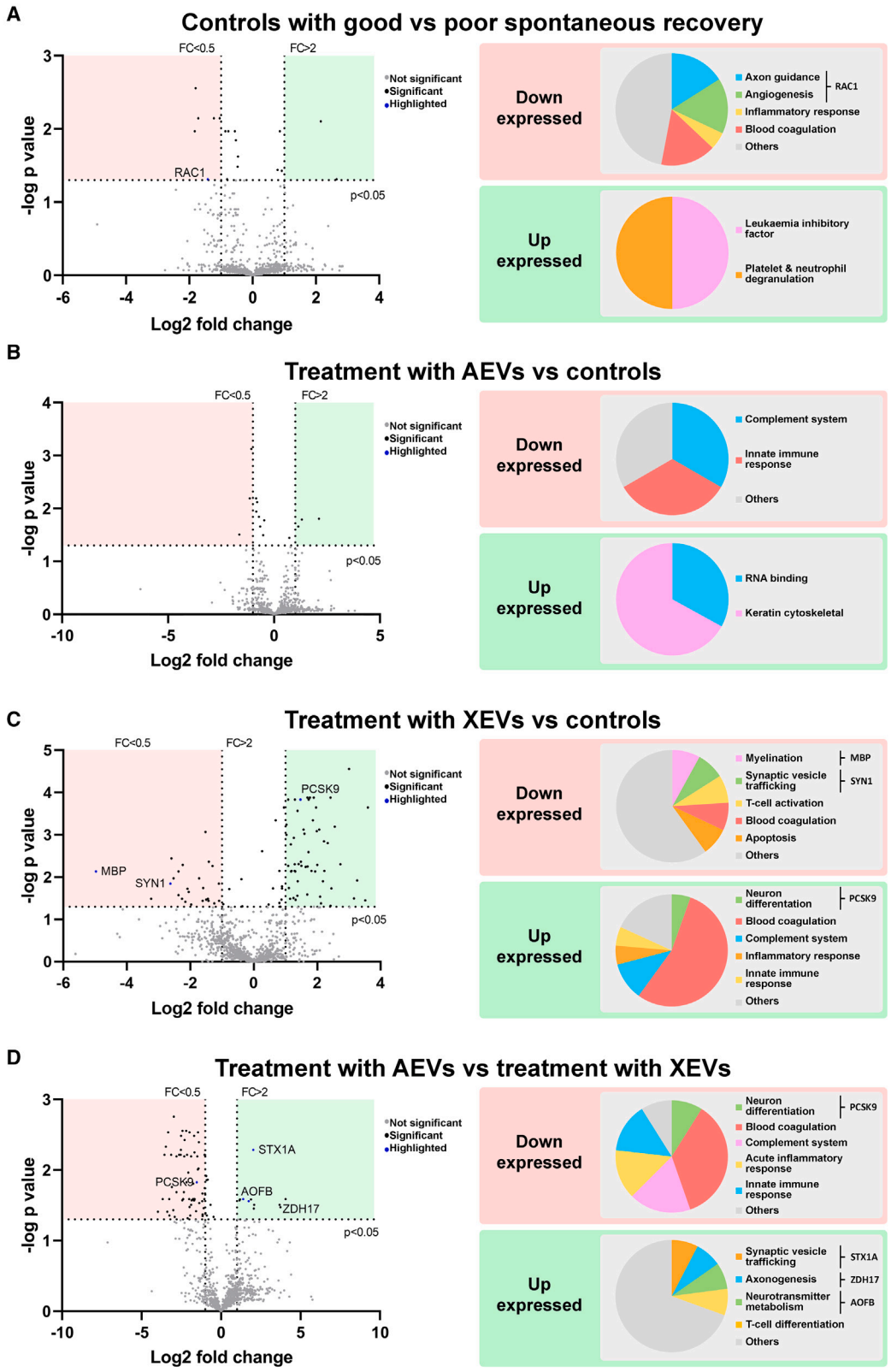

(legend on next page)

PROS, and KNT2 (blood coagulation); FCN1, C1QB, and MASP2 (complement system); C1QA and C1S (complement activation); THRB, CO9, and CO4 (blood coagulation and complement activation); LAC2 and IGHG1 (B cell receptor signaling pathway and complement system); HPT, A1AT, and A2MG (inflammatory response); IGG2C and IGHD (innate immune response); PCSK9 (neuron differentiation); SPA3N, TFR1, and CERU (cellular iron ion homeostasis); LIFR (leukemia inhibitory factor signaling pathway); and HBB1 and HBA (erythrocyte development).

DISCUSSION

This study shows that allogeneic and xenogenic blood-derived EVs from rats with spontaneous recovery and from patients with remarkable recovery after an ICH improve functional outcomes, white matter integrity, and histological markers of tissue repair in an animal model of ICH, with no immune system activation or malignancies. These findings, based on a novel approach that uses EVs harvested from subjects with spontaneous recovery as a treatment in a proof-of-concept study, support the hypothesis that EVs act as mediators of biological processes of protection and repair after an ICH. Also, the intravenous administration of these EVs appears to be safe. The proteomics study of the circulating EVs in the post-acute stage showed differential protein expression in animals with good vs. poor recovery and in treated animals that had better functional outcomes and showed superior markers of recovery compared with the controls. A number of the differential proteins observed appear to be involved in biological pathways related to mechanisms of neural protection and repair, such as axon guidance, angiogenesis (RAC1), synaptic vesicle trafficking (SYN1 and STX1A), angiogenesis (ZDH17), neuron differentiation (PCSK9), myelination (MBP), and immune system activation pathways (CO4, KLKB1, PROC, FA9 and C1QA). These results open a window of opportunity to deepen the knowledge of the metabolic pathways associated with recovery toward the development of new therapies for ICH.

There is an urgent need to find effective treatments to reduce the burden of ICH. Although there has been no translation into successful therapies, various therapeutic approaches are being explored in preclinical models of ICH.[3] Stem cell-based therapies such as MSCs reduce brain injury and improve recovery after ICH.[5–7] More recently, stem cell-derived EVs have been proposed as the effectors of the beneficial effect of such therapies; MSC-derived EVs are therefore emerging as a substitute for the cell therapy itself.[23,24] EVs have certain advantages over stem cells, such as less immunogenicity related to the low presence of major histocompatibility complex I and II on the surface,[25–30] EVs can cross the blood-brain barrier and have a low risk of secondary microvascular thrombosis and occlusion after systemic administration.[31,32] It has been shown that EVs are distributed not only in brain but in other organs such as lung, liver, and spleen in the first 24 h after intravenous administration.[21,33] This spread biodistribution does not affect the efficacy of EVs as treatment in preclinical models of ischemic stroke.[21,34] Our results suggest that, in fact, circulating EVs released after ICH are involved in recovery mechanisms, results that are in line with previous studies that showed the capacity of MSC-derived EVs to reduce functional impairment after ICH.[30,35] Although, this study did not investigate the cellular origin of the blood-derived EVs, it is highly likely that these vesicles might originate not only from stem cells but also from other cell lines in a systemic response to the brain injury that involves intercellular signaling. In fact, an immune systemic response is involved in secondary injury cascades after bleeding into the brain.[36,37] Also, the release of EVs from neural cells and astrocytes has been shown to enhance brain plasticity and inhibit the mechanisms of damage after a stroke.[38,39] We focused our study on blood-derived EVs and their content, which might reflect all the processes involved in such a systemic response as a whole, to provide information on the biological processes underlying brain damage and repair after ICH.

We chose various surrogate biomarkers of recovery and repair to increase the consistency of our results and therefore included the functional evaluation of animals with three assessment scales,[40–43] imaging biomarkers of fibers and white matter integrity such as DTI-FA[44] and immunofluorescence of various molecular biomarkers of brain repair.[21] Those we chose included MOG, OLIG-2, GFAP, and VEFG. ICH affects white matter and axon integrity, leading to myelin loss.[45,46] An important myelin marker is the glycoprotein MOG, which is located on the surface of myelin sheaths in the central nervous system and has been proposed to participate in cellular adhesion.[47,48] Another important marker of white matter integrity is OLIG-2, a nuclear transcription factor related to the phenotype definition of the oligodendroglial lineage.[49] In our study, the administration of AEVs and XEVs was associated with a greater MOG immunofluorescence signal compared with the control animals, while OLIG-2 levels were increased only in the AEVs-treated animals. Together with data from DTI-FA, these results suggest that treatment with EVs actually improves myelin sheath preservation and that AEVs increase oligodendrocyte maturation. These results deserve further studies to identify the content of both types of EVs used as treatment, in order to determine the molecules that may act as effectors of recovery.

GFAP has been suggested as a specific marker of astrocyte activation. In response to a stroke, astrocytes are activated to produce a glial scar, aimed at protecting the healthy tissue from further secondary injury

Figure 5. Protein content in EVs and outlining of their metabolic pathways

Proteins and pathways up-expressed are marked in green, and those down-expressed in red. The volcano plots represent proteins present in EVs by study group comparisons. Biological pathways in which the differential proteins appear to be involved are shown in the pie charts on the right. Some biological pathways considered to be theoretically less involved in damage or repair mechanisms were grouped as "others" to ease the graphic representation of data (e.g., erythrocyte development, integrin signaling). (A) Control animals with good vs. poor spontaneous recovery. (B) Treated animals with AEVs vs. controls. (C) XEVs-treated vs. control animals. (D) AEVs-treated vs. XEVs-treated animals. AEVs, allogeneic extracellular vesicles; FC, fold change; XEVs, xenogenic extracellular vesicles.

cascades.[50] However, astrocyte overactivation might inhibit axonal regeneration,[51] increasing cerebral inflammation, and can result in blood-brain barrier breakdown.[52] An inflammatory response together with aberrant astrocyte proliferation and further neuronal loss surrounding the damaged area has been reported at 7 days after an ICH.[53] In this study, GFAP expression was lower in the perilesional area in both treatment groups compared with the controls, suggesting a modulation of astroglial activation that might act in favor of reducing neuronal loss and improving axonal regeneration.

The study of histological markers related to the vascular system, such as VEGF, is considered of relevance in animal models of stroke. VEGF is an angiogenic factor that is essential in neovascularization, vascular permeability, and oxygen delivery processes.[54] In this study, no differences were found in VEGF expression between the study groups, which is not surprising because reduced blood and oxygen supply are not key factors in the pathophysiology of brain damage after ICH. Neovascularization and enhancement of vascular permeability would therefore not be targets for the biological processes of protection and repair.

When investigating novel therapeutic approaches, safety also needs to be verified. We therefore assessed the plasma expression of cytokines and chemokines to rule out an immune response to EVs treatment. The only findings occurred in the XEVs-treated rats that showed a slight increase in IL-6 at 6 h together with a decrease in CXCL1 during the first 24 h after treatment. IL-6 is a pro-inflammatory cytokine involved in immune responses, and CXCL1 is involved in recruiting neutrophils as a response to external injuries.[55,56] These changes were considered to be related to the xenogenic origin of the EVs, were transient, returned to normal after 24 h, and were not associated with any sign of disease in the treated animals. Interestingly no anti-inflammatory cytokines or chemokines were found. In addition, no malignancies were observed in the long term, at 3 months after treatment, with either of the treatments. In addition, it has been reported that EVs can contribute to thrombotic events due to the proteins located on the surface,[57] but no complications related to thrombotic effects were observed in the animals during the experiment. In light of these results, we can conclude that EVs treatment appears to be safe.

Considering that proteins are fundamental effectors of biological functions, we also studied the differential protein cargo of circulating EVs from animals in the predefined study groups as biomarkers of the processes underlying the different outcomes among groups and to address whether circulating EVs might be involved in enhancement of the mechanisms of protection and repair after treatment. As recently described, circulating EVs following an experimental ICH in rats show higher expression of proteins related to healing and removal of debris and repair processes at 28 days compared with baseline.[58]

Regarding spontaneous good and poor recovery, it is remarkable that EVs from animals with good recovery had shown a lower content of proteins related to inflammation and cellular iron homeostasis,[59] which might indicate less activation of secondary injury cascades.[36] The protein RAC1, which is related to axon guidance pathways[60] and axonal regeneration,[61] had also been less present in the EVs from the animals with good functional recovery after 28 days, which might indicate a lower need for activation of such pathways.

Second, to analyze the effect of EVs administered to animals as a treatment, both treated groups were compared with the control group. Although differential protein expression was observed between the AEV-treated and control animals, we could not identify biological pathways clearly related to injury or repair mechanisms that could explain the beneficial effects observed in the AEV-treated group. There is a possibility that certain biological functions have not been identified using current databases or even that certain relevant proteins have not been identified. Nevertheless, the observed differences deserve further investigation.

Regarding the protein content of the EVs in the animals treated with XEVs compared with those from the control group, several proteins involved in the pathways potentially related to mechanisms of protection or repair were found up-expressed in the treated animals. PCSK9 is involved in regulating neuronal apoptosis, in neurogenesis, and in neuron differentiation[62] and enhancement of these mechanisms could be related to the improvement in tissue preservation and motor performance observed in treated animals. Myelin (MBP) and synaptogenic (SYN1) proteins were found down-expressed, which probably reflects a lower need to activate mechanisms for remyelinization and synaptogenesis in better preserved tissue. In contrast, proteins involved in immune response and complement activation pathways were found up-expressed in the treated animals. A xenogenic product was administered as a treatment, and although only a slight immune reaction was observed in the safety study, a certain degree of immune response expressed in the circulating EVs cannot be completely ruled out.

Last, we compared the AEV- and XEV-treated animals to explore the differences in response according to EVs origin. Compared with those in the XEVs-treated group, the AEVs-treated animals had circulating EVs whose cargo displayed up-expression of proteins involved in pathways related to synaptic function, such as synaptic vesicle trafficking (STX1A),[63,64] axonogenesis (ZDH17),[65] and neurotransmitter metabolism (AOFB),[66,67] whereas in the XEVs-treated animals, the EVs expressed PCSK9 protein related to the regulation of neuronal apoptosis, neurogenesis, and neuron differentiation pathways.[62] These findings might indicate activation of different pathways potentially involved in the mechanisms of protection and repair depending on the origin of the EVs used as treatment.

This study has three main limitations. First, the recommended isolation protocols describe ultracentrifugation as one of the best methods for isolating EVs.[68,69] Due to the limited individual volume of the samples from the rats, however, other isolating methods (with less sample but contrasting results) had to be used during the study. Second, it would have been interesting to obtain EVs after treatment to

have data for at least two different time points to analyze the changes in the proteomic content of EVs according to outcomes. Last, for the proteomics analysis, EVs samples were introduced as a unique pool per group, limiting the natural variance of individual samples. Future study designs should approach singular variances by using individual or different pools of samples from the same group. Also, the proteomics technique itself has certain limitations that need to be considered. Libraries are indispensable for sequential window acquisition of all theoretical mass spectra (SWATH-MS) analysis, and not all known proteins are located in a single library; moreover, there can be proteins in samples not identified by proteomics because their peptides are more hydrophilic or hydrophobic or because these peptides are masked by other larger peptides. So far, locating the most interesting library is challenging and might include confounding proteins that hinder the discovery of proteins.

Conclusions

The results of this study suggest that blood-derived EVs are involved in enhancing mechanisms of protection and repair post-ICH and improve functional recovery. The administration of blood-derived EVs, regardless of origin, is safe. These findings open a new and promising opportunity for further development of restorative therapies to improve outcomes of patients with ICH. The specific role of the proteins described as possibly related to repair mechanisms and their therapeutic potential deserve further investigation in future studies.

MATERIAL AND METHODS

This was an experimental study to explore the efficacy and safety of EVs treatment in a rat model of ICH. The experiments were performed at the Neurological Sciences and Cerebrovascular Research Laboratory, Neurology and Cerebrovascular Disease Group, Neuroscience Area of IdiPAZ Health Research Institute, La Paz University Hospital, Madrid, Spain.

Ethics statement

All experimental procedures were designed to minimize animal suffering in compliance with and approved by the Ethics Committee for the Care and Use of Animals in Research (Ref. PROEX 159/17) according to Spanish and European Union (EU) regulations ([86/609/CEE, 2003/65/CE, and 2010/63/EU] and Spanish Royal Decrees [RD 1201/2005 and RD53/2013]). Experiments were conducted according to the Stroke Therapy Academic Industry Roundtable (STAIR),[70] RIGOR,[71] and HEADS[4] recommendations guidelines in terms of randomization and statistical powering.

The study in humans was approved by the Ethics Committee of La Paz University Hospital. All patients or their proxies provided their informed consent to participate (PI-3093).

Experimental procedure

Sprague-Dawley rats (8–9 weeks old, weighing 225–275 g) were used throughout the study. Anesthesia was induced using an anesthetic chamber with 8% sevoflurane in a 1 L/min oxygen flow and maintained with 4% sevoflurane in a 1 L/min oxygen flow through a facial mask. After an intraperitoneal injection of meloxidyl (2 mg/mL) (Ceva, France), the animals were placed in a stereotaxic frame to induce an ICH in the striatum. A craniotomy was performed adjacent to the bregma, and the following stereotaxic coordinates for the injection site with respect to the bregma were used as previously described: 0.04 mm posterior, 3.5 mm lateral, and 6.0 mm ventral.[7] The hemorrhage was induced by injecting 1 μL of saline containing 0.5 U of collagenase type IV (Sigma-Aldrich, USA). The presence and location of the ICH was verified by MRI at 48 h.

The rats were euthanized for histological study at 28 days post-ICH by an intracardial injection of potassium chloride. The brains were fixed by immersion in 4% paraformaldehyde for 24 h and 30% sucrose for 72 h and stored at −80°C in optimum cutting temperature compound (Sakura, USA) until the experiments were performed.

Experimental study protocol

The study protocol is summarized in Figure 6 and consisted of an efficacy study and a safety study. For the efficacy study, both male and female animals were included (proportion of 1:1) and allocated to the following groups: (1) healthy group (10 rats without surgery and no treatment); (2) sham group (10 rats subjected to surgery without ICH induction and saline administration as a treatment); (3) control group (20 rats subjected to ICH and saline administration); (4) allogeneic EVs treatment (AEVs) group (10 rats subjected to ICH and AEVs administration); and (5) xenogenic EVs treatment (XEVs) group (10 rats subjected to ICH and XEVs administration). Rats in the AEVs and XEVs groups were allocated randomly. For the safety study, male and female animals (proportion of 1:1) were allocated to the following groups: AEVs group (6 rats administered AEVs) and XEVs group (6 rats with XEVs administration).

To obtain the treatments.

- AEVs were obtained from blood samples (1 mL) collected at 7 days post-ICH from the rats in the control group and those from the animals that showed a spontaneous good recovery at 28 days were used as treatment. We selected as donors of AEVs the animals that reached the highest scores (within the first tertile) in all the three tests used for functional assessment explained below (Rogers', RotaRod, and tapered beam walking tests).
- XEVs were obtained from blood samples collected at 7 days from symptom onset from patients with spontaneous ICH of supratentorial location admitted to the Department of Neurology and Stroke Center of La Paz University Hospital, Madrid, Spain, and treated according to the current clinical protocols. EVs from the patients who showed a remarkable good outcome at 6 months, defined as >10 points or >50% improvement from the baseline National Institute of Health Stroke Scale score and modified Rankin Scale score ≤ 2, were selected to be used as treatment.

All treatments (saline, AEVs, and XEVs) were administered intravenously through the tail vein at 24 h after ICH induction.

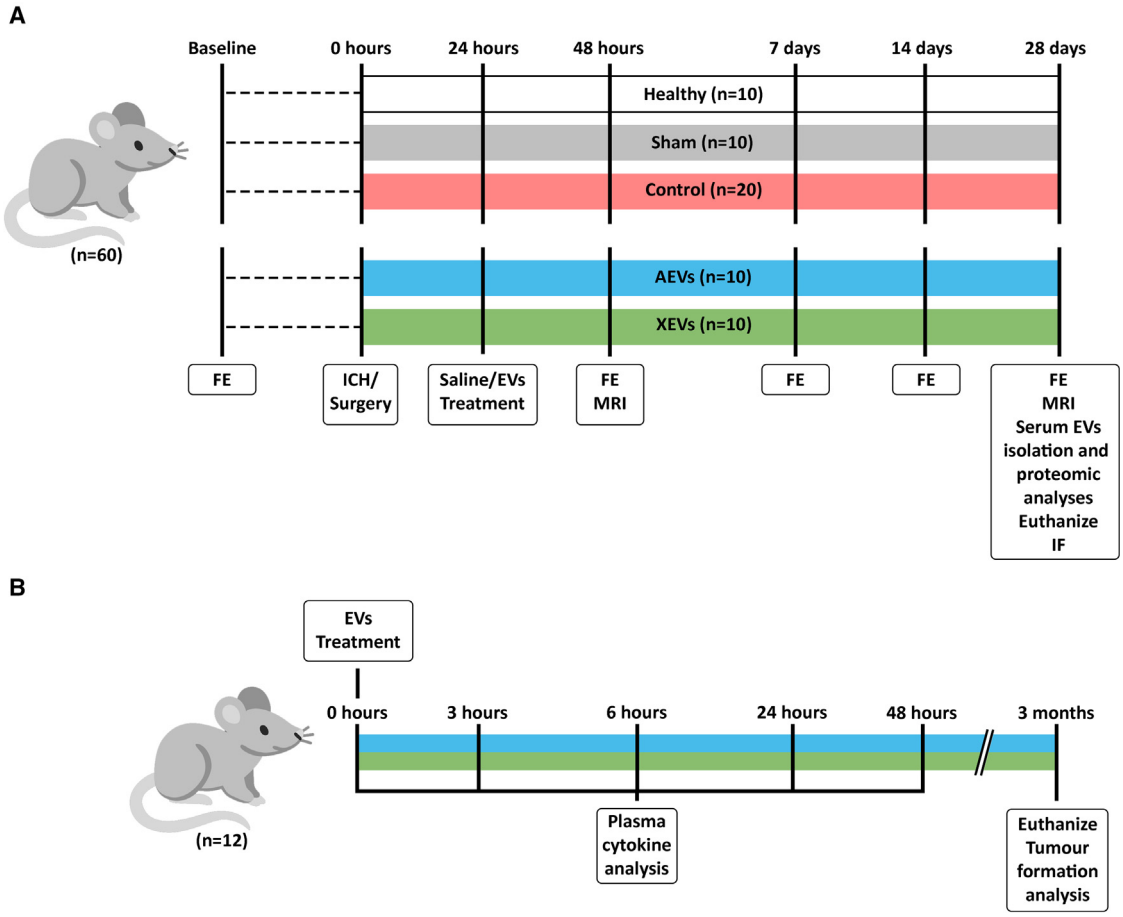

Figure 6. Experimental procedure schemes

(A) Design of the efficacy study. (B) Design of the safety study. AEVs, allogeneic EVs; EVs, extracellular vesicles; FE, functional evaluation; IF, immunofluorescence; MRI, magnetic resonance imaging; XEVs, xenogenic EVs.

EVs isolation and characterization

For all study purposes, EVs were isolated from serum. Blood samples were centrifuged at 3,000 × *g* for 15 min at 4°C. The ExoQuick Ultra EVs isolation kit (System Biosciences, USA) was used following the manufacturer's instructions. This method first precipitates EVs with other compounds such as albumin and immunoglobulin (Ig).[72] The purification column then removes IgG, albumin, and other proteins by affinity chromatography. Samples with isolated EVs were then stored at −80°C until analysis.

For the EVs characterization, three different methods were used: (1) western blot; (2) transmission electron microscopy (TEM); and (3) nanoparticle tracking analysis (NTA).

(1) Western blot was performed, using a 4%–10% sodium dodecyl sulphate-polyacrylamide gel for electrophoresis, with 20 μg of protein per lane. The following specific EVs antibodies were used: anti-Alix (1:1,000, Cell Signal, USA), anti-CD63 (1:1,000, Abcam, UK), and anti-CD81 (1:1,000, Abcam, UK). Anti-Albumin (1:1,000, Abcam, UK) antibody was used as a purity control. This was then followed by horseradish peroxidase (HRP) secondary antibody (1:10,000, Abcam). Image acquisition was performed with ECL Pierce chemiluminescence (Thermo Fisher Scientific, USA) in an image acquisition system (Uvitec, UK).

(2) TEM was used to visualize EVs and verify their size (30–200 nm). The EVs were fixed in 2.5% glutaraldehyde 0.1 M sodium cacodylate solution for 1 h at 4°C and fixed with 2%-osmium tetroxide for 1 h at 4°C. The EVs pellet was dehydrated with a graded acetone series and then embedded in resin. Thick sections of 60 nm were cut and observed under TEM at 80 kV.

(3) The size and number of EVs were analyzed through an NTA using a NanoSight LN10 instrument (Malvern Instruments, UK). EVs were diluted in 500 μL of sterile phosphate-buffered saline for a working concentration of 1×10^7–10^9 particles/mL and 60 s videos were recorded at a shutter speed of 30.00 ms and a camera level of 13. For the analyses, a detection threshold of 3 was employed, which was performed in triplicate.

Those EVs harvested from rats or humans at 7 days to be used as AEVs or XEVs treatments were pooled after the previously described isolation and characterization procedures. Treatment consisted of 100 μg of the total protein present, measured by a Pierce BCA Protein Assay Kit (Thermo Fisher Scientific, USA) diluted in 1 mL saline for intravenous administration in a single dose as shown in the study protocol (Figure 6A). EVs obtained at 28 days in all study groups were used to analyze differences in the protein cargo depending on outcomes.

Outcomes

The efficacy assessments included a functional evaluation, white matter integrity, and fiber density assessed by DTI-FA in MRI, and histological markers of brain repair by immunofluorescence (Figure 6A). All evaluations were performed by blinded observers.

Functional assessment scales

Functional assessments were performed prior to surgery (baseline) and at 48 h, 7 days, 14 days, and 28 days post-ICH. The assessment included the following:

(1) A variant of the Rogers' test,[40] scored as follows: 0 = no functional deficit; 1 = failure to fully extend the forepaw; 2 = decreased forelimb grip while the tail is gently pulled; 3 = spontaneous movement in all directions, contralateral circling only if pulled by the tail; 4 = circling; 5 = walking only when stimulated; 6 = unresponsive to stimulation with a depressed level of consciousness; and 7 = dead.
(2) The RotaRod test,[41] which evaluates the rats' capacity to remain on a rotating cylinder at constant acceleration, from 4 to 40 rpm for 2 min. The total time in the cylinder before falling was recorded, with longer times associated with better performance.
(3) The tapered beam walking test,[42,43] which evaluates the rats' ability to traverse a wooden beam without the affected hindlimb slipping. A higher slip ratio, calculated using the formula {[total slips + (0.5 × half-slips)]/total steps} × 100%, reflects poorer performance.

MRI and fractional anisotropy

The presence and location of the hemorrhage was confirmed by T2-weighted spin-echo MRI at 48 h post-ICH and the residual lesion at 28 days using a 7 T horizontal bore magnet (Bruker Pharmascan, Germany). Images were acquired with a rapid acquisition with relaxation enhancement (RARE) sequence in axial orientations and with the following parameters: number of echo images 2 (echo time [TE]: 29.54 ms and 88.61 ms), repetition time (TR) = 3,000 ms, RARE factor = 4, Av = 3, field of view (FOV) = 3.5 cm, acquisition matrix = 256 × 256 corresponding to an in-plane resolution of 137 × 137 μm^2, slice thickness = 1.00 mm without a gap and number of slices = 16. To estimate the total volume of the ICH lesion, the formula of the ellipsoid volume was used: A×B×C/2, where A is the greatest hemorrhage diameter in the coronal plane, B the hemorrhage diameter at 90° to diameter A in the coronal plane and C the greatest hemorrhage diameter in the sagittal plane. Values are shown in mm^3. Since MRI images in the acute phase does not allow to separate the hematoma itself from the associated edema, the volume of the lesion measured includes both. This correlates with stain postmortem sections of the brain.[73]

DTI-FA maps were obtained at 28 days as a biomarker of fiber density and myelination of white matter. Images were obtained in 30 different diffusion encoding gradient directions using a multi-shot spin-echo planar imaging sequence. The acquisition conditions were a diffusion gradient duration = 3 ms; diffusion gradient separation = 18 ms; TR = 8,000 ms; TE = 67 ms, FOV = 3.8 cm; axial slices of 1.5 mm thickness and 2b values = 500 and 1,000 s/mm^2; acquisition matrix = 128 × 128. The region of interest (ROI) in the DTI-FA maps was located in the section where the largest lesion was seen. To normalize the fractional anisotropy (FA) values, the ROI of the lesion was divided by the same ROI in the contralateral side, and the value was expressed as relative FA values, by a blinded observer.

Immunofluorescence for histological markers of brain damage and repair

The peri-hemorrhage area was studied using immunofluorescence in 10-μm-thick brain slices. MOG (1:50, Millipore, USA) and oligodendrocyte nuclei with OLIG-2 (1:450, Millipore, USA) were used as markers of myelin preservation, and GFAP (1:500, Millipore, USA) was used as a marker of astrocytes in the perilesional zone. Angiogenesis was studied with VEGF (1:500, Millipore, USA), followed by goat anti-mouse and anti-rabbit Alexa Fluor 488 (1:750, Invitrogen, USA). Immunofluorescence images were acquired with a DMI 4000 B confocal microscope (Leica, Germany), using a ×40 objective lens, and analyzed using LAS AF software (Leica, Germany). The mean fluorescence intensity of the ROI was measured by the NIS-Element AR (Nikon, Japan) 4.5 Program. Assessments were performed using the same microscope configurations to eliminate bias due to background normalization.

Safety assessment

To confirm the treatments' safety, two approaches were considered (Figure 6B).

(1) Analysis of the immune system activation by determining levels of pro- and anti-inflammatory cytokines in plasma at baseline and at 3 h, 6 h, 24 h, and 48 h after treatment. Levels of IL-6, CXCL1 (KC), IL-10, IFN-γ, CCL2 (MCP-1), TNF-α, granulocyte-macrophage colony-stimulating factor, IL-18, IL-12p70, IL-1β, IL-1α, IL-17A, and IL-33 were measured using the LEGENDplex Rat Inflammation Panel (BioLegend, USA), according to the manufacturer's instructions. Data were acquired on a FACSCalibur cytometer (BD Biosciences, USA) and analyzed using the LEGENDplex Data Analysis Software Suite (Qognit Inc, USA).
(2) The presence or absence of tumor formation in organs. Macroscopic and microscopic observations were performed on the brain, lungs, heart, liver, spleen, and kidneys at 3 months post-treatment. The organs were fixed in 4% paraformaldehyde for 24 h, 30% sucrose for 72 h, and stored at -80°C in optimum

cutting temperature compound (Sakura, USA) until assessment. Sections 10 μm thick every 50 μm were cut to analyze nonhomogeneous cell aggregations in a CM1950 cryostat (Leica, Germany). For H&E staining, sections were immersed for 10 s in hematoxylin (Thermo Fisher Scientific, USA) and then for 30 s in eosin (Sigma-Aldrich, USA). The sections were then dehydrated and coverslipped with DPX mounting medium (Merk, USA). Staining was observed using an Axio microscope (Zeiss, Germany) with a ×40 objective lens and processed by Image-Pro Plus 4.1 (Media Cybernetics, USA).

All evaluations were made by blinded observers.

Proteomic analysis of the EVs content

A mass spectrometric data-dependent acquisition (DDA) qualitative analysis and protein quantification by SWATH-MS data independent acquisition (DIA) was performed to determine the specific protein content of EVs at 28 days in the study groups. To perform a qualitative and quantitative protein identification, an equal amount of protein (100 μg) was processed. Peptides of 4 μg were digested and separated using reverse phase chromatography. The gradient was created using the micro-liquid chromatography system nano LC 400 (SCIEX, USA) coupled to a high-speed Triple TOF 6600 mass spectrometer (SCIEX, USA) with a microflow source using a DDA method. Proteins were identified using a rat-specific Uniprot database.[74] For this analysis, only those proteins with an FDR <1% (99% protein confidence) were selected. For the relative quantification by the SWATH-MS DIA method, we first built a spectral library grouping each EVs type in a pool. Then 4 μg of each sample was run and their technical replicates (three samples, each one run per triplicate) in the TripleTOF 6600 using an SWATH-MS acquisition method.[75] For detailed explanation of the proteomic acquisition, see supplemental materials. The total ion chromatogram profile for each individual sample used in the DDA method and qualitative and quantitative SWATH-MS analysis are shown in the supplemental material.

Proteins showing differences at the significance level of an adjusted p value < 0.05 and a more than 2-fold change (FC) (up-expressed) or less than 0.5 FC (down-expressed) were considered as having a differential expression between groups (see statistical analysis section for further details on the comparisons). The biological pathways in which those proteins are involved were identified based on the Uniprot database.[74] The mass spectrometry proteomics data have been deposited to the ProteomeXchange Consortium via the PRIDE[76] partner repository with the dataset identifier PRIDE: PXD038630.

Statistical analysis

The power analysis showed that, with non-parametric testing for behavioral tests and immunofluorescence, at least 10 rats needed to be randomly assigned to each group for a significance level of 5% (alpha) and a power of 80% (1 - beta).

The results are expressed as mean ± standard deviation (SD). For the tissue integrity analyses of DTI-FA, the data were compared using an analysis of variance adjusted to Tukey's method for normally distributed data. For immune response, functional evaluation, ICH volume, and immunofluorescence analyses, the data were compared using the Kruskal-Wallis test followed by the Mann-Whitney *U* test. p values < 0.05 were considered statistically significant at a 95% confidence interval. Analyses were performed using SPSS 23 (IBM, USA), and the figures were obtained using GraphPad Prism 8 (GraphPad software, USA).

The results from the proteomics studies were analyzed using SWATH-MS principal components analysis (PCA) and cluster analysis, R 3.5.3 (R Core Team, Austria) and "base," "stats," "gplots," "Hmisc," "dplyr," and "car" packages. The PCA was applied, taking into account the correlation matrix due to its pairwise two-sided p values being 0 for the entire matrix, and therefore all of them are statistically significant, which could explain the good success in applying the PCA. The total variability of the data was 87.70% and is explained with the first two principal components. For the cluster analysis, Student's t test for means comparison between samples was previously applied and used Euclidean distance, suitable for quantitative variables and complete linkage as cluster criteria. For differentially expressed protein selection, p values were adjusted using a Benjamini-Hochberg correction, and proteins with an FC > 2 or <0.5 and an adjusted p value < 0.05 were selected.

DATA AVAILABILITY

All data generated or analyzed during this study are included in this published article and its supplemental material.

SUPPLEMENTAL INFORMATION

Supplemental information can be found online at https://doi.org/10.1016/j.omtn.2023.03.006.

ACKNOWLEDGMENTS

The experimental animal model study was approved by the Ethics Committee for Research in Animals at the La Paz University Hospital and authorized by the Madrid Regional Government. Animal care and experimental procedures were designed in accordance with our medical school's Ethical Committee for the Care and Use of Animals in Research (Ref. PROEX 159/17) according to the Spanish (RD 1201/2005 and RD53/2013) and EU (86/609/CEE, 2003/65/CE, and 2010/63/EU) rules.

This work was supported by Instituto de Salud Carlos III (ISCIII) and co-funded by the European Union (European Regional Development Fund -FEDER) under grant PI17/01922 and PI20/00243; Invictus plus network under grant RD16/0019/0005; RICORS network under grant RD21/0006/0012; Miguel Servet under grant CP15/00069 and CPII20/00002 to M.G.-F. and CP20/00024 to L.O.-O.; Sara Borrell under grant CD19/00033 to M.P.-M., CD20/00112 to M.d.P.C.-V. and CD21/00059 to J.A.-O.; Ministerio de Universidades, Plan de Recuperación, Transformación y Resiliencia, Universidad Autónoma de Madrid under grant CA1/RSUE/2021-00753 to D.P.-A.; and the Spanish Ministry of Health-ISCIII under grant FI18/00026 to F.L.-G. and FI17/00188 to M.C.G.-d.F.

We appreciate the editing assistance of Morote Traducciones S.L.

AUTHOR CONTRIBUTIONS

M.G.-F. and M.AL. conceived the study, designed and reviewed the experiments, analyzed results, obtained funding, made the critical review of the manuscript and approved it for submission. F.L.-G., L.C.-F., and D.P. performed and analyzed the experiments and drafted the manuscript. M.C.G.-d.F. and J.K.A.-E. performed histological studies. M.P.-M. and E.A.-L. performed functional evaluation scales. J.A.-O. and E.L.-C. performed safety studies. L.O.-O. assisted in EVs characterization. S.B.B. and M.P.C.-V. conducted the proteomics studies. M.I.L.-H. and A.G.-P. assisted in the analysis and interpretation of proteomics. B.F. and E.D.-T. assisted in the review and interpretation of results. All authors discussed and approved the final version of the manuscript.

DECLARATION OF INTERESTS

A.G.-P. is a shareholder of Biomedica Molecular Medicine SL.

REFERENCES

1. Krishnamurthi, R.V., Feigin, V.L., Forouzanfar, M.H., Mensah, G.A., Connor, M., Bennett, D.A., Moran, A.E., Sacco, R.L., Anderson, L.M., Truelsen, T., et al. (2013). Global and regional burden of first-ever ischaemic and haemorrhagic stroke during 1990–2010: findings from the Global Burden of Disease Study 2010. Lancet. Glob. Health *1*, e259–e281. https://doi.org/10.1016/S2214-109X(13)70089-5.
2. GBD 2016 Stroke Collaborators, Nguyen, M., Roth, G.A., Nichols, E., Alam, T., Abate, D., Abd-Allah, F., Abdelalim, A., Abraha, H.N., Abu-Rmeileh, N.M., et al. (2019). Global, regional, and national burden of stroke, 1990–2016: a systematic analysis for the Global Burden of Disease Study 2016. Lancet Neurol. *18*, 439–458. https://doi.org/10.1016/S1474-4422(19)30034-1.
3. Crilly, S., Withers, S.E., Allan, S.M., Parry-Jones, A.R., and Kasher, P.R. (2021). Revisiting promising preclinical intracerebral hemorrhage studies to highlight repurposable drugs for translation. Int. J. Stroke *16*, 123–136. https://doi.org/10.1177/1747493020972240.
4. Hemorrhagic Stroke Academia Industry HEADS Roundtable Participants (2018). Basic and translational Research in intracerebral hemorrhage: limitations, priorities, and recommendations. Stroke *49*, 1308–1314. https://doi.org/10.1161/STROKEAHA.117.019539.
5. Huang, A.P.H., Hsu, Y.H., Wu, M.S., Tsai, H.H., Su, C.Y., Ling, T.Y., Hsu, S.H., and Lai, D.M. (2020). Potential of stem cell therapy in intracerebral hemorrhage. Mol. Biol. Rep. *47*, 4671–4680. https://doi.org/10.1007/S11033-020-05457-9.
6. Hu, Y., Liu, N., Zhang, P., Pan, C., Zhang, Y., Tang, Y., Deng, H., Aimaiti, M., Zhang, Y., Zhou, H., et al. (2016). Preclinical studies of stem cell transplantation in intracerebral hemorrhage: a systemic review and meta-analysis. Mol. Neurobiol. *53*, 5269–5277. https://doi.org/10.1007/S12035-015-9441-6.
7. Otero, L., Zurita, M., Bonilla, C., Aguayo, C., Vela, A., Rico, M.A., and Vaquero, J. (2011). Late transplantation of allogeneic bone marrow stromal cells improves neurologic deficits subsequent to intracerebral hemorrhage. Cytotherapy *13*, 562–571. https://doi.org/10.3109/14653249.2010.544720.
8. Chen, J., Venkat, P., Zacharek, A., and Chopp, M. (2014). Neurorestorative therapy for stroke. Front. Hum. Neurosci. *8*, 382. https://doi.org/10.3389/FNHUM.2014.00382.
9. Kusuma, G.D., Carthew, J., Lim, R., and Frith, J.E. (2017). Effect of the microenvironment on mesenchymal stem cell paracrine signaling: opportunities to engineer the therapeutic effect. Stem Cell. Dev. *26*, 617–631. https://doi.org/10.1089/SCD.2016.0349.
10. Harrell, C.R., Fellabaum, C., Jovicic, N., Djonov, V., Arsenijevic, N., and Volarevic, V. (2019). Molecular mechanisms responsible for therapeutic potential of mesenchymal stem cell-derived secretome. Cells *8*, 467. https://doi.org/10.3390/CELLS8050467.
11. Ge, L., Xun, C., Li, W., Jin, S., Liu, Z., Zhuo, Y., Duan, D., Hu, Z., Chen, P., and Lu, M. (2021). Extracellular vesicles derived from hypoxia-preconditioned olfactory mucosa mesenchymal stem cells enhance angiogenesis via miR-612. J. Nanobiotechnol. *19*, 380. https://doi.org/10.1186/S12951-021-01126-6.
12. Admyre, C., Johansson, S.M., Qazi, K.R., Filén, J.J., Lahesmaa, R., Norman, M., Neve, E.P.A., Scheynius, A., and Gabrielsson, S. (2007). Exosomes with immune modulatory features are present in human breast milk. J. Immunol. *179*, 1969–1978. https://doi.org/10.4049/JIMMUNOL.179.3.1969.
13. Carnino, J.M., Lee, H., and Jin, Y. (2019). Isolation and characterization of extracellular vesicles from Broncho-Alveolar lavage fluid: a review and comparison of different methods. Respir. Res. *20*, 240–311. https://doi.org/10.1186/S12931-019-1210-Z.
14. Brenna, S., Altmeppen, H.C., Mohammadi, B., Rissiek, B., Schlink, F., Ludewig, P., Krisp, C., Schlüter, H., Failla, A.V., Schneider, C., et al. (2020). Characterization of brain-derived extracellular vesicles reveals changes in cellular origin after stroke and enrichment of the prion protein with a potential role in cellular uptake. J. Extracell. Vesicles *9*, 1809065. https://doi.org/10.1080/20013078.2020.1809065.
15. Rybak, K., and Robatzek, S. (2019). Functions of extracellular vesicles in immunity and virulence. Plant Physiol. *179*, 1236–1247. https://doi.org/10.1104/PP.18.01557.
16. Shen, H., Yao, X., Li, H., Li, X., Zhang, T., Sun, Q., Ji, C., and Chen, G. (2018). Role of exosomes derived from miR-133b modified MSCs in an experimental rat model of intracerebral hemorrhage. J. Mol. Neurosci. *64*, 421–430. https://doi.org/10.1007/S12031-018-1041-2.
17. Otero-Ortega, L., Laso-García, F., Gómez-de Frutos, M., Fuentes, B., Diekhorst, L., Díez-Tejedor, E., and Gutiérrez-Fernández, M. (2019). Role of exosomes as a treatment and potential biomarker for stroke. Transl. Stroke Res. *10*, 241–249. https://doi.org/10.1007/S12975-018-0654-7.
18. Chen, K.H., Chen, C.H., Wallace, C.G., Yuen, C.M., Kao, G.S., Chen, Y.L., Shao, P.L., Chen, Y.L., Chai, H.T., Lin, K.C., et al. (2016). Intravenous administration of xenogenic adipose-derived mesenchymal stem cells (ADMSC) and ADMSC-derived exosomes markedly reduced brain infarct volume and preserved neurological function in rat after acute ischemic stroke. Oncotarget *7*, 74537–74556. https://doi.org/10.18632/ONCOTARGET.12902.
19. Xin, H., Li, Y., Cui, Y., Yang, J.J., Zhang, Z.G., and Chopp, M. (2013). Systemic administration of exosomes released from mesenchymal stromal cells promote functional recovery and neurovascular plasticity after stroke in rats. J. Cerebr. Blood Flow Metabol. *33*, 1711–1715. https://doi.org/10.1038/jcbfm.2013.152.
20. Xin, H., Li, Y., Liu, Z., Wang, X., Shang, X., Cui, Y., Zhang, Z.G., and Chopp, M. (2013). MiR-133b promotes neural plasticity and functional recovery after treatment of stroke with multipotent mesenchymal stromal cells in rats via transfer of exosome-enriched extracellular particles. Stem Cell. *31*, 2737–2746. https://doi.org/10.1002/STEM.1409.
21. Otero-Ortega, L., Laso-García, F., Gómez-de Frutos, M.D.C., Rodríguez-Frutos, B., Pascual-Guerra, J., Fuentes, B., Díez-Tejedor, E., and Gutiérrez-Fernández, M. (2017). White matter repair after extracellular vesicles administration in an experimental animal model of subcortical stroke. Sci. Rep. *7*, 44433–44511. https://doi.org/10.1038/srep44433.
22. Doeppner, T.R., Herz, J., Görgens, A., Schlechter, J., Ludwig, A.-K., Radtke, S., de Miroschedji, K., Horn, P.A., Giebel, B., and Hermann, D.M. (2015). Extracellular vesicles improve post-stroke neuroregeneration and prevent postischemic immunosuppression. Stem Cells Transl. Med. *4*, 1131–1143. https://doi.org/10.5966/SCTM.2015-0078/-/DC1.
23. Huang, Y.-C., and Lai, L.-C. (2019). The potential roles of stem cell-derived extracellular vesicles as a therapeutic tool. Ann. Transl. Med. *7*, 693. https://doi.org/10.21037/ATM.2019.11.66.
24. Wiklander, O.P.B., Brennan, M., Lötvall, J., Breakefield, X.O., and El Andaloussi, S. (2019). Advances in therapeutic applications of extracellular vesicles. Sci. Transl. Med. *11*, eaav8521. https://doi.org/10.1126/SCITRANSLMED.AAV8521.
25. Schu, S., Nosov, M., O'Flynn, L., Shaw, G., Treacy, O., Barry, F., Murphy, M., O'Brien, T., and Ritter, T. (2012). Immunogenicity of allogeneic mesenchymal stem cells. J. Cell Mol. Med. *16*, 2094–2103. https://doi.org/10.1111/J.1582-4934.2011.01509.X.
26. Synowsky, S.A., Shirran, S.L., Cooke, F.G.M., Antoniou, A.N., Botting, C.H., and Powis, S.J. (2017). The major histocompatibility complex class I immunopeptidome

of extracellular vesicles. J. Biol. Chem. *292*, 17084–17092. https://doi.org/10.1074/JBC.M117.805895.

27. Gowen, A., Shahjin, F., Chand, S., Odegaard, K.E., Yelamanchili, S.V., Petty, H.R., Xiong, G., Fok, E., Gowen, A., Shahjin, F., et al. (2020). Mesenchymal stem cell-derived extracellular vesicles: challenges in clinical applications. Front. Cell Dev. Biol. *8*, 149. https://doi.org/10.3389/FCELL.2020.00149.

28. Lai, R.C., Arslan, F., Lee, M.M., Sze, N.S.K., Choo, A., Chen, T.S., Salto-Tellez, M., Timmers, L., Lee, C.N., El Oakley, R.M., et al. (2010). Exosome secreted by MSC reduces myocardial ischemia/reperfusion injury. Stem Cell Res. *4*, 214–222. https://doi.org/10.1016/J.SCR.2009.12.003.

29. Lee, M., Ban, J.J., Yang, S., Im, W., and Kim, M. (2018). The exosome of adipose-derived stem cells reduces β-amyloid pathology and apoptosis of neuronal cells derived from the transgenic mouse model of Alzheimer's disease. Brain Res. *1691*, 87–93. https://doi.org/10.1016/J.BRAINRES.2018.03.034.

30. Otero-Ortega, L., Laso-García, F., Gómez-de Frutos, M.C., Diekhorst, L., Martínez-Arroyo, A., Alonso-López, E., García-Bermejo, M.L., Rodríguez-Serrano, M., Arrúe-Gonzalo, M., Díez-Tejedor, E., et al. (2020). Low dose of extracellular vesicles identified that promote recovery after ischemic stroke. Stem Cell Res. Ther. *11*, 70. https://doi.org/10.1186/S13287-020-01601-1.

31. Cai, J., Wu, J., Wang, J., Li, Y., Hu, X., Luo, S., and Xiang, D. (2020). Extracellular vesicles derived from different sources of mesenchymal stem cells: therapeutic effects and translational potential. Cell Biosci. *10*, 1–14. https://doi.org/10.1186/S13578-020-00427-X.

32. Banks, W.A., Sharma, P., Bullock, K.M., Hansen, K.M., Ludwig, N., and Whiteside, T.L. (2020). Transport of extracellular vesicles across the blood-brain barrier: brain pharmacokinetics and effects of inflammation. Int. J. Mol. Sci. *21*, 4407. https://doi.org/10.3390/IJMS21124407.

33. Kang, M., Jordan, V., Blenkiron, C., and Chamley, L.W. (2021). Biodistribution of extracellular vesicles following administration into animals: a systematic review. J. Extracell. Vesicles *10*, e12085. https://doi.org/10.1002/JEV2.12085.

34. Thomas, J.M., Cunningham, C.J., Lawrence, C.B., Pinteaux, E., and Allan, S.M. (2020). Therapeutic potential of extracellular vesicles in preclinical stroke models: a systematic review and meta-analysis. BMJ Open Sci. *4*, e100047. https://doi.org/10.1136/bmjos-2019-100047.

35. Han, Y., Seyfried, D., Meng, Y., Yang, D., Schultz, L., Chopp, M., and Seyfried, D. (2018). Multipotent mesenchymal stromal cell–derived exosomes improve functional recovery after experimental intracerebral hemorrhage in the rat. J. Neurosurg. *131*, 290–300. https://doi.org/10.3171/2018.2.JNS171475.

36. Bai, Q., Xue, M., and Yong, V.W. (2020). Microglia and macrophage phenotypes in intracerebral haemorrhage injury: therapeutic opportunities. Brain *143*, 1297–1314. https://doi.org/10.1093/BRAIN/AWZ393.

37. Zhang, J., Shi, K., Li, Z., Li, M., Han, Y., Wang, L., Zhang, Z., Yu, C., Zhang, F., Song, L., et al. (2018). Organ- and cell-specific immune responses are associated with the outcomes of intracerebral hemorrhage. Faseb. J. *32*, 220–229. https://doi.org/10.1096/FJ.201700324R.

38. Li, M., Li, X., Wang, D., Gao, X., Li, S., Cheng, X., Shen, Y., Li, S., Jia, Q., and Liu, Q. (2021). Inhibition of exosome release augments neuroinflammation following intracerebral hemorrhage. Faseb. J. *35*, e21617. https://doi.org/10.1096/FJ.202002766R.

39. Xin, H., Wang, F., Li, Y., Lu, Q.E., Cheung, W.L., Zhang, Y., Zhang, Z.G., and Chopp, M. (2017). Secondary release of exosomes from astrocytes contributes to the increase in neural plasticity and improvement of functional recovery after stroke in rats treated with exosomes harvested from MicroRNA 133b-overexpressing multipotent mesenchymal stromal cells. Cell Transplant. *26*, 243–257. https://doi.org/10.3727/096368916X693031.

40. Rogers, D.C., Campbell, C.A., Stretton, J.L., and Mackay, K.B. (1997). Correlation between motor impairment and infarct volume after permanent and transient middle cerebral artery occlusion in the rat. Stroke *28*, 2060–2065. https://doi.org/10.1161/01.STR.28.10.2060.

41. Zarruk, J.G., García-Yébenes, I., Romera, V.G., Ballesteros, I., Moraga, A., Cuartero, M.I., Hurtado, O., Sobrado, M., Pradillo, J.M., Fernández-López, D., et al. (2011). Neurological tests for functional outcome assessment in rodent models of ischaemic stroke. Rev. Neurol. *53*, 607–618. https://doi.org/10.33588/rn.5310.2011016.

42. Boltze, J., Lukomska, B., and Jolkkonen, J.; MEMS–IRBI consortium (2014). Mesenchymal stromal cells in stroke: improvement of motor recovery or functional compensation? J. Cerebr. Blood Flow Metabol. *34*, 1420–1421. https://doi.org/10.1038/JCBFM.2014.94.

43. Schallert, T., Woodlee, M., and Fleming, S. (2002). Disentangling multiple types of recovery from brain injury. Pharmacol Cereb Ischemia *2002*, 201–216.

44. Son, J.P., Sung, J.H., Kim, D.H., Cho, Y.H., Kim, S.J., Chung, J.W., Chang, W.H., Kim, Y.H., Kim, E.H., Moon, G.J., and Bang, O.Y. (2021). Brain morphological and connectivity changes on MRI after stem cell therapy in a rat stroke model. PLoS One *16*, e0246817–e0246818. https://doi.org/10.1371/journal.pone.0246817.

45. Fu, X., Zhou, G., Zhuang, J., Xu, C., Zhou, H., Peng, Y., Cao, Y., Zeng, H., Li, J., Yan, F., et al. (2021). White matter injury after intracerebral hemorrhage. Front. Neurol. *12*, 562090. https://doi.org/10.3389/FNEUR.2021.562090.

46. Liu, Y., Lu, G., Su, X.W., Ding, T., Wang, W.L., Li, Y.M., Poon, W.S., and Ao, L.J. (2018). Characterization of axon damage, neurological deficits, and histopathology in two experimental models of intracerebral hemorrhage. Front. Neurosci. *12*, 928. https://doi.org/10.3389/FNINS.2018.00928.

47. Quarles, R.H. (1997). Glycoproteins of myelin sheaths. J. Mol. Neurosci. *8*, 1–12. https://doi.org/10.1007/BF02736858.

48. Johns, T.G., and Bernard, C.C. (1999). The structure and function of myelin oligodendrocyte glycoprotein. J. Neurochem. *72*, 1–9. https://doi.org/10.1046/J.1471-4159.1999.0720001.X.

49. Yokoo, H., Nobusawa, S., Takebayashi, H., Ikenaka, K., Isoda, K., Kamiya, M., Sasaki, A., Hirato, J., and Nakazato, Y. (2004). Anti-human Olig2 antibody as a useful immunohistochemical marker of normal oligodendrocytes and gliomas. Am. J. Pathol. *164*, 1717–1725. https://doi.org/10.1016/S0002-9440(10)63730-3.

50. Liu, Z., and Chopp, M. (2016). Astrocytes, therapeutic targets for neuroprotection and neurorestoration in ischemic stroke. Prog. Neurobiol. *144*, 103–120. https://doi.org/10.1016/J.PNEUROBIO.2015.09.008.

51. Stern, S., Hilton, B.J., Burnside, E.R., Dupraz, S., Handley, E.E., Gonyer, J.M., Brakebusch, C., and Bradke, F. (2021). RhoA drives actin compaction to restrict axon regeneration and astrocyte reactivity after CNS injury. Neuron *109*, 3436–3455.e9. https://doi.org/10.1016/J.NEURON.2021.08.014.

52. Zhang, L., Lei, Z., Guo, Z., Pei, Z., Chen, Y., Zhang, F., Cai, A., Mok, G., Lee, G., Swaminathan, V., et al. (2020). Development of neuroregenerative gene therapy to reverse glial scar tissue back to neuron-enriched tissue. Front. Cell. Neurosci. *14*, 594170. https://doi.org/10.3389/FNCEL.2020.594170.

53. Masuda, T., Maki, M., Hara, K., Yasuhara, T., Matsukawa, N., Yu, S., Bae, E.C., Tajiri, N., Chheda, S.H., Solomita, M.A., et al. (2010). Peri-hemorrhagic degeneration accompanies stereotaxic collagenase-mediated cortical hemorrhage in mouse. Brain Res. *1355*, 228–239. https://doi.org/10.1016/J.BRAINRES.2010.07.101.

54. Zheng, J., Sun, J., Yang, L., Zhao, B., and Fan, Z. (2017). The potential role of vascular endothelial growth factor as a new biomarker in severe intracerebral hemorrhage. J. Clin. Lab. Anal. *31*, e22076. https://doi.org/10.1002/jcla.22076.

55. Tanaka, T., Narazaki, M., and Kishimoto, T. (2014). IL-6 in inflammation, immunity, and disease. Cold Spring Harbor Perspect. Biol. *6*, a016295. https://doi.org/10.1101/CSHPERSPECT.A016295.

56. Sawant, K.V., Poluri, K.M., Dutta, A.K., Sepuru, K.M., Troshkina, A., Garofalo, R.P., and Rajarathnam, K. (2016). Chemokine CXCL1 mediated neutrophil recruitment: role of glycosaminoglycan interactions. Sci. Rep. *6*, 33123–33128. https://doi.org/10.1038/srep33123.

57. Zarà, M., Guidetti, G.F., Camera, M., Canobbio, I., Amadio, P., Torti, M., Tremoli, E., and Barbieri, S.S. (2019). Biology and role of extracellular vesicles (EVs) in the pathogenesis of thrombosis. Int. J. Mol. Sci. *20*, 2840. https://doi.org/10.3390/IJMS20112840.

58. Laso-García, F., Piniella, D., Gómez-de Frutos, M.C., Casado-Fernández, L., Pérez-Mato, M., Alonso-López, E., Otero-ortega, L., Bravo, S.B., Chantada-Vázquez, M.D.P., Trilla-fuertes, L., et al. (2022). Protein content of blood-derived extracellular vesicles : an approach to the pathophysiology of cerebral hemorrhage. Front. Cell. Neurosci. *16*, 1058546. https://doi.org/10.3389/fncel.2022.1058546.

59. Hua, Y., Keep, R.F., Hoff, J.T., and Xi, G. (2007). Brain injury after intracerebral hemorrhage: the role of thrombin and iron. Stroke *38*, 759–762. https://doi.org/10.1161/01.STR.0000247868.97078.10.

60. Hua, Z.L., Emiliani, F.E., and Nathans, J. (2015). Rac1 plays an essential role in axon growth and guidance and in neuronal survival in the central and peripheral nervous systems. Neural Dev. *10*, 21. https://doi.org/10.1186/S13064-015-0049-3.

61. Bu, F., Min, J.W., Munshi, Y., Lai, Y.J., Qi, L., Urayama, A., McCullough, L.D., and Li, J. (2019). Activation of endothelial ras-related C3 botulinum toxin substrate 1 (Rac1) improves post-stroke recovery and angiogenesis via activating Pak1 in mice. Exp. Neurol. *322*, 113059. https://doi.org/10.1016/J.EXPNEUROL.2019.113059.

62. Seidah, N.G., Benjannet, S., Wickham, L., Marcinkiewicz, J., Jasmin, S.B., Stifani, S., Basak, A., Prat, A., and Chrétien, M. (2003). The secretory proprotein convertase neural apoptosis-regulated convertase 1 (NARC-1): liver regeneration and neuronal differentiation. Proc. Natl. Acad. Sci. USA *100*, 928–933. https://doi.org/10.1073/PNAS.0335507100.

63. Singer-Lahat, D., Sheinin, A., Chikvashvili, D., Tsuk, S., Greitzer, D., Friedrich, R., Feinshreiber, L., Ashery, U., Benveniste, M., Levitan, E.S., and Lotan, I. (2007). K+ channel facilitation of exocytosis by dynamic interaction with syntaxin. J. Neurosci. *27*, 1651–1658. https://doi.org/10.1523/JNEUROSCI.4006-06.2007.

64. Singer-Lahat, D., Chikvashvili, D., and Lotan, I. (2008). Direct interaction of endogenous Kv channels with syntaxin enhances exocytosis by neuroendocrine cells. PLoS One *3*, e1381. https://doi.org/10.1371/JOURNAL.PONE.0001381.

65. Shi, W., Wang, F., Gao, M., Yang, Y., Du, Z., Wang, C., Yao, Y., He, K., Chen, X., and Hao, A. (2015). ZDHHC17 promotes axon outgrowth by regulating TrkA-tubulin complex formation. Mol. Cell. Neurosci. *68*, 194–202. https://doi.org/10.1016/J.MCN.2015.07.005.

66. Birgner, C., Kindlundh-Högberg, A.M.S., Oreland, L., Alsiö, J., Lindblom, J., Schiöth, H.B., and Bergström, L. (2008). Reduced activity of monoamine oxidase in the rat brain following repeated nandrolone decanoate administration. Brain Res. *1219*, 103–110. https://doi.org/10.1016/J.BRAINRES.2008.05.014.

67. Falk, E.M., Cook, V.J., Nichols, D.E., and Sprague, J.E. (2002). An antisense oligonucleotide targeted at MAO-B attenuates rat striatal serotonergic neurotoxicity induced by MDMA. Pharmacol. Biochem. Behav. *72*, 617–622. https://doi.org/10.1016/S0091-3057(02)00728-1.

68. Veerman, R.E., Teeuwen, L., Czarnewski, P., Güclüler Akpinar, G., Sandberg, A., Cao, X., Pernemalm, M., Orre, L.M., Gabrielsson, S., and Eldh, M. (2021). Molecular evaluation of five different isolation methods for extracellular vesicles reveals different clinical applicability and subcellular origin. J. Extracell. Vesicles *10*, e12128. https://doi.org/10.1002/JEV2.12128.

69. Brennan, K., Martin, K., FitzGerald, S.P., O'Sullivan, J., Wu, Y., Blanco, A., Richardson, C., and Mc Gee, M.M. (2020). A comparison of methods for the isolation and separation of extracellular vesicles from protein and lipid particles in human serum. Sci. Rep. *10*, 1039–1113. https://doi.org/10.1038/s41598-020-57497-7.

70. Fisher, M., Feuerstein, G., Howells, D.W., Hurn, P.D., Kent, T.A., Savitz, S.I., and Lo, E.H.; STAIR Group (2009). Update of the stroke therapy academic industry roundtable preclinical recommendations. Stroke *40*, 2244–2250. https://doi.org/10.1161/STROKEAHA.108.541128.

71. Lapchak, P.A., Zhang, J.H., and Noble-Haeusslein, L.J. (2013). RIGOR guidelines: escalating STAIR and STEPS for effective translational Research. Transl. Stroke Res. *4*, 279–285. https://doi.org/10.1007/s12975-012-0209-2.

72. Coughlan, C., Bruce, K.D., Burgy, O., Boyd, T.D., Michel, C.R., Garcia-Perez, J.E., Adame, V., Anton, P., Bettcher, B.M., Chial, H.J., et al. (2020). Exosome isolation by ultracentrifugation and precipitation and techniques for downstream analyses. Curr. Protoc. cell Biol. *88*, e110–e154. https://doi.org/10.1002/CPCB.110.

73. Del Bigio, M.R., Yan, H.J., Buist, R., and Peeling, J. (1996). Experimental intracerebral hemorrhage in rats. Magnetic resonance imaging and histopathological correlates. Stroke *27*, 2312–2319. https://doi.org/10.1161/01.STR.27.12.2312.

74. UniProt Consortium (2021). UniProt: the universal protein knowledgebase in 2021. Nucleic Acids Res. *49*, D480–D489. https://doi.org/10.1093/nar/gkaa1100.

75. Chantada-Vázquez, M.D.P., García Vence, M., Serna, A., Núñez, C., and Bravo, S.B. (2021). SWATH-MS protocols in human diseases. Methods Mol. Biol. *2259*, 105–141. https://doi.org/10.1007/978-1-0716-1178-4_7.

76. Perez-Riverol, Y., Bai, J., Bandla, C., García-Seisdedos, D., Hewapathirana, S., Kamatchinathan, S., Kundu, D.J., Prakash, A., Frericks-Zipper, A., Eisenacher, M., et al. (2022). The PRIDE database resources in 2022: a hub for mass spectrometry-based proteomics evidences. Nucleic Acids Res. *50*, D543–D552. https://doi.org/10.1093/NAR/GKAB1038.